Selective Desorption of Alkanethiols in Mixed Self-Assembled Monolayers for Subsequent Oligonucleotide Attachment and DNA Hybridization

Munlika Satjapipat, Raymond Sanedrin, and Feimeng Zhou*

Department of Chemistry and Biochemistry, California State University, Los Angeles, California 90032

Received June 27, 2001. In Final Form: September 5, 2001

Oligonucleotides whose 5′ ends are linked to mercaptohexyl tether groups (HS-ss-DNA) are attached onto gold regions freshly exposed by reductive desorption of the mercaptopropionic acid (MPA) in a mixed MPA/hexanethiol (HT) or MPA/mercaptohexanol (MCH) self-assembled monolayer (SAM). The size of the bare Au region was shown to be controllable by using various MPA/HT solution compositions during the fabrication of the mixed SAMs. Atomic force microscopy shows that the size of the segregated gold regions has a profound effect on the surface density and orientation of the subsequently immobilized HS-ss-DNA molecules. The DNA surface density begins to increase when the bare gold domain (12−19 nm wide, prepared by stripping MPA off a mixed SAM formed from a solution with an alkanethiol molar ratio of $\chi_{MPA}/\chi_{HT} = 1/4$) approaches the size of the HS-ss-DNA (ca. 5−6 nm for a 17mer). The surface density of the HS-ss-DNA in the mixed HS-ss-DNA/HT SAM or the mixed HS-ss-DNA/MCH SAM is slightly greater than SAMs containing only the HS-ss-DNA, but the orientation of the HS-ss-DNA in the mixed SAM is more favorable for DNA hybridization. The quartz crystal microbalance (QCM) responses for the DNA hybridization at the DNA SAMs and mixed SAMs of HS-ss-DNA and alkanethiol formed using various adsorption methods were compared. The mixed HS-ss-DNA/HT formed using the new method resulted in a QCM signal amplification by almost 1 order of magnitude over SAMs containing only the HS-ss-DNA, with a much improved hybridization efficiency (ca. 96%).

1. Introduction

Mixed self-assembled monolayers (SAMs) composed of alkanethiols of different chain lengths offer a controllable route for constructing moieties containing different chemical functionalities.[1−5] Mixed SAMs are model systems for studies of adsorption,[6] wetting,[7] and heterogeneous electron transfer[8−10] and have led to important applications in the development of biosensors[11,12] such as heterogeneous DNA/RNA sensors[13−31] and preparation of biologically important surfaces.[32] It has been well established that coadsorption of two alkanethiols of different chain lengths on gold is thermodynamically controlled, and the resultant two-component monolayers do not phase-segregate into macroscopic islands (islands of submicrometers).[3,4] Recent studies based on scanning probe microscopy, however, have revealed that domains rich in individual components can be observed in the range of several tens of nanometers.[33−36] One of the consequences of the nanometer-sized phase separation is that alkanethiols of varying chain

(1) Kumar, A.; Abbott, N. L.; Kim, E.; Biebuyck, H. A.; Whitesides, G. M. *Acc. Chem. Res.* **1995**, *28*, 219−226.
(2) Ullman, A. *An Introduction to Ultrathin Organic Films: From Langmuir−Blodgett to Self-Assembly*; Academic Press: Boston, 1991.
(3) Bain, C. D.; Evall, J.; Whitesides, G. M. *J. Am. Chem. Soc.* **1989**, *111*, 7155−7164.
(4) Bain, C. D.; Whitesides, G. M. *J. Am. Chem. Soc.* **1989**, *111*, 7164−7175.
(5) Chidsey, C. E. D. *Science* **1991**, *251*, 919−922.
(6) Prime, K. L.; Whitesides, G. M. *Science* **1991**, *252*, 1164−1167.
(7) Ullman, A.; Evans, S. D.; Shnidman, Y.; Sharma, R.; Eilers, J. E.; Chang, J. C. *J. Am. Chem. Soc.* **1991**, *113*, 1499−1506.
(8) Richardson, J. N.; Peck, S. R.; Curtin, L. S.; Tender, L. M.; Terrill, R. H.; Carter, M. T.; Murray, R. W.; Rowe, G. K.; Creager, S. E. *J. Phys. Chem.* **1995**, *99*, 766−772.
(9) Rowe, G. K.; Carter, M. T.; Richardson, J. N.; Murray, R. W. *Langmuir* **1995**, *11*, 1797−1806.
(10) Chidsey, C. E. D.; Bertozzi, C. R.; Putvinski, T. M.; Mujsce, A. M. *J. Am. Chem. Soc.* **1990**, *112*, 4301−4306.
(11) Janata, J.; Josowicz, M.; Vanysek, P.; DeVaney, M. D. *Anal. Chem.* **1998**, *70*, 179R−208R.
(12) Wink, T.; van Zuilen, S. J.; Bult, A.; van Bennekom, W. P. *Analyst* **1997**, *122*, 43R−50R.
(13) Wang, J.; Palecek, E.; Nielsen, P.; Rivas, G.; Cai, X.; Shiraishi, H.; Dontha, N.; Luo, D.; Farias, P. *J. Am. Chem. Soc.* **1996**, *118*, 7667−7670.
(14) Wang, J.; Nielsen, P. E.; Jiang, M.; Cai, X.; Fernades, J. R.; Grant, D. H.; Ozsoz, M.; Beglieter, A.; Mowart, M. *Anal. Chem.* **1997**, *69*, 5200−5202.
(15) Wang, J.; Rivas, G.; Jiang, M.; Zhang, X. *Langmuir* **1999**, *15*, 6541−6545.
(16) Wang, J.; Jiang, M.; Mukherjee, B. *Bioelectrochem. Bioenerg.* **2000**, *52*, 111−114.
(17) Thompson, M.; Furtado, L. M. *Analyst* **1999**, *124*, 1133−1136.
(18) Furtado, L. M.; Su, H.; Thompson, M.; Mack, D. P.; Hayward, G. L. *Anal. Chem.* **1999**, *71*, 1167−1175.
(19) Cavic, B. A.; Hayward, G. L.; Thompson, M. *Analyst* **1999**, *124*, 1405−1420.
(20) Steel, A. B.; Levicky, R. L.; Herne, T. M.; Tarlov, M. J. *Biophys. J.* **2000**, *79*, 975−981.
(21) Steel, A. B.; Herne, T. M.; Tarlov, M. J. *Anal. Chem.* **1998**, *70*, 4670−4677.
(22) Levicky, R.; Herne, T. M.; Tarlov, M. J.; Satija, S. K. *J. Am. Chem. Soc.* **1998**, *120*, 9787−9792.
(23) Georgiadis, R.; Peterlinz, K. P.; Peterson, A. W. *J. Am. Chem. Soc.* **2000**, *122*, 3166−3173.
(24) Nelson, B. P.; Grimsrud, T. E.; Liles, M. R.; Goodman, R. M.; Corn, R. M. *Anal. Chem.* **2001**, *73*, 1−7.
(25) Thiel, A. J.; Frutos, A. G.; Jordan, C. E.; Corn, R. M.; Smith, L. M. *Anal. Chem.* **1997**, *69*, 4948−4956.
(26) He, L.; Musick, M. D.; Nicewarner, S. R.; Salinas, F. G.; Benkovic, S. J.; Natan, M. J.; Keating, C. D. *J. Am. Chem. Soc.* **2000**, *122*, 9071−9077.
(27) Patolsky, F.; Ranjit, K. T.; Lichtenstein, A.; Willner, I. *Chem. Commun.* **2000**, 1025−1026.
(28) Patolsky, F.; Lichtenstein, A.; Willner, I. *J. Am. Chem. Soc.* **2000**, *122*, 418−419.
(29) O'Brien, J. C.; Stickney, J. T.; Porter, M. D. *J. Am. Chem. Soc.* **2000**, *122*, 5004−5005.
(30) Okahata, Y.; Matsunobu, Y.; Ijiro, K.; Mukae, M.; Murakami, A.; Makino, K. *J. Am. Chem. Soc.* **1992**, *114*, 8299−8300.
(31) Hegner, M.; Dreier, M.; Wagner, P.; Semenza, G.; Guntherodt, J. J. *J. Vac. Sci. Technol., B* **1996**, 1419−1421.
(32) Whitesides, G. M.; Bain, C. D. *Science* **1988**, *240*, 62−63.
(33) Stranick, S. J.; Parikh, A. N.; Tao, Y.-Y.; Allara, D. L.; Weiss, P. S. *J. Phys. Chem.* **1994**, *98*, 7636−7646.

10.1021/la010989i CCC: $20.00 © 2001 American Chemical Society
Published on Web 10/26/2001

lengths can be electrochemically desorbed in alkaline media at different potentials.[34,37−40]

Selective desorption of one component in a mixed SAM, therefore, should be a viable means to form nanometer-sized gold regions dispersed in the matrix of the other alkanethiol component. If a different species can be attached onto the freshly exposed gold region at a rate faster than the surface diffusion of the remaining alkanethiol, the newly formed hybrid system should also possess phase separation with similar domain sizes. Since surface diffusion of alkanethiols to defects[41] or patterns created by scanning probe lithography[42] was shown to take many hours, the reattachment of a different species into these nanometer-sized domains is possible so long as the immobilization process is facile. For example, Hobora et al. have shown that the domain sizes after the selective replacement of 3-mercaptopropionic acid are approximately equal to that of the initial phase-separated 1-undecanethiol and 3-mercaptopropionic acid mixed SAM. We envisioned that the attachment of DNA into such nanometer-scaled domains may offer certain unique surface features and should shed light on the fundamental understanding of SAMs of DNA[20−22,43−47] and their possible applications as sequence-specific heterogeneous DNA sensors.[13−19,24,25,27−31,43−54] Moreover, the surface orientation of the mercaptohexyl tether groups (HS-ss-DNA) might be tunable by carefully controlling the size of the segregated gold regions and judiciously choosing an alkanethiol suitable to organize the HS-ss-DNA probes. When properly designed, one would expect that mixed HS-ss-DNA/alkanethiol SAMs can be produced with a high surface density and an ordered structure.[20−22,43] Both aspects are known to be important factors affecting the DNA hybridization at the surface/solution interface. The consideration of reorienting these surface-confined oligonucleotides with an alkanethiol is inspired by the work of Tarlov and co-workers who utilized an alkanethiol to competitively replace those nonspecifically adsorbed HS-ss-DNA molecules.[20−22,43,48] The competitive adsorption step was deemed necessary since many of the HS-ss-DNA molecules tend to be nonspecifically adsorbed via the interaction of the DNA bases with the gold surface.

In this work, we explored the possibility of selectively desorbing an alkanethiol in a mixed SAM for subsequent oligonucleotide probe immobilization and target hybridization. We examined the effect of the composition of the mixed SAMs on the dimensions of the segregated gold regions. Emphasis was placed on the examination of the HS-ss-DNA surface coverage and orientation in the gold region whose dimension becomes comparable to the size of the HS-ss-DNA probe. Cyclic voltammetry, magnetically alternating current atomic force microscopy (MAC-AFM), and flow injection quartz crystal microbalance (FI-QCM) were used in tandem to study the selective desorption process and the subsequent HS-ss-DNA attachment to the freshly exposed gold regions. We also attempted to delineate the relationship between the extent of DNA hybridization/hybridization efficiency and the surface coverage/orientation of the HS-ss-DNA in the mixed SAMs. The advantages of the mixed HS-ss-DNA/alkanethiol SAM prepared with our method were compared to SAMs containing only HS-ss-DNA and mixed HS-ss-DNA/alkanethiol SAMs prepared through immersing the HS-ss-DNA-covered Au surface in an alkanethiol solution for the replacement of the nonspecifically adsorbed HS-ss-DNA molecules (referred to as the competitive alkanethiol replacement procedure for the remainder of the text).

2. Experimental Section

Materials. Hexanethiol (HT), mercaptopropionic acid (MPA), and mercaptohexanol (MCH) were all obtained from Aldrich Chemicals. $HClO_4$, NaOH, and NaCl (Fisher Scientific) were used as received. EDTA and Tris·HCl were purchased from Sigma. Water used for solution preparation was treated with a Millipore water purification system. A thiolated 17mer probe (SH-$(CH_2)_6$-5′-GTAAAACGACGGCCAGT-3′), a thiolated 15mer probe (SH-$(CH_2)_6$-5′-GCGCGCGCGCGCGCG-3′), and the target with a sequence complementary to the 17mer probe were all acquired from Integrated DNA Technologies, Inc. (Coralville, IA).

Solution Preparation. TE buffer solutions (10 mM Tris·HCl and 1 mM EDTA) had a pH of 7.0, and the TE/NaCl (TNE) solutions had a NaCl concentration of 0.1 M. The probe and target solution preparation followed our published procedure.[52] MPA, MCH, and HT solutions were prepared by diluting stock solutions with water to different molar ratios with a total alkanethiol concentration of 2 mM.

Electrodes and Substrates. Gold(111) films evaporated on mica were either purchased from Molecular Imaging Inc. (Phoenix, AZ) or generously provided by Dr. N. Tao (Arizona State University). A Pt wire was used as the counter electrode, and a Ag wire coated with AgCl was employed as a quasi reference electrode for the electrochemical AFM experiments. The Au-coated QCM crystals had a fundamental frequency of 7.995 MHz (5 mm in diameter, ICM Technologies, Oklahoma City, OK).

Instrumentation. AFM images were collected with an AFM equipped with a MAC mode and a bipotentiostat (both from Molecular Imaging Inc.). Cyclic voltammetry and QCM measurements were performed using a CHI 440 electrochemical quartz crystal microbalance (EQCM, CH Instrument, Austin, TX). The flow injection quartz crystal microbalance (FI-QCM) and the experimental protocol have been described in our previous work.[52,55]

Procedures. (a) AFM. The mixed MPA/HT or MPA/MCH SAMs were prepared by soaking the clean substrate into the MPA/HT solution overnight. Three different molar ratios between MPA and HT (χ_{MPA}/χ_{HT} = 4/1, 1/1, and 1/4) and the molar ratio

(34) Hobara, D.; Takayuki, S.; Imabayashi, S.-I.; Kakiuchi, T. *Langmuir* **1999**, *15*, 5073−5078.
(35) Folkers, J. P.; Laibinis, P. E.; Whitesides, G. M. *Langmuir* **1992**, *8*, 133−1341.
(36) Tamada, K.; Hara, M.; Sasabe, H.; Knoll, W. *Langmuir* **1997**, *13*, 1558−1566.
(37) Porter, M. D.; Weisshaar, D. E.; Lamp, B. D. *J. Am. Chem. Soc.* **1992**, *114*, 5860−5862.
(38) Walczak, M. M.; Popenoe, D. D.; Deinhammer, R. S.; Lamp, B. D.; Chung, C.; Porter, M. D. *Langmuir* **1991**, *7*, 2687−2693.
(39) Imahayahshi, S.-I.; Gon, N.; Sasaki, N.; Hobara, D.; Kakiuchi, T. *Langmuir* **1998**, *14*, 2348−2351.
(40) Kawaguchi, T.; Yasuda, H.; Shimazu, K.; Porter, M. D. *Langmuir* **2000**, *16*, 9830−9840.
(41) Zamborini, F. P.; Crooks, R. M. *Langmuir* **1998**, *14*, 3279−3286.
(42) Schoer, J. K.; Crooks, R. M. *Langmuir* **1997**, *13*, 2323−2332.
(43) Herne, T. M.; Tarlov, M. J. *J. Am. Chem. Soc.* **1997**, *119*, 8916−8920.
(44) Demers, L. M.; Mirkin, C. A.; Mucic, R. C.; Reynolds, R. A. I.; Letsinger, R. L.; Elgahanian, R.; Viswanadham, G. *Anal. Chem.* **2000**, *72*, 5535−5541.
(45) Kelley, S. O.; Barton, J. K.; Jackson, N. M.; Hill, M. G. *Bioconjugate Chem.* **1997**, *8*, 31−37.
(46) Hartwich, G.; Caruana, D. J.; de Lumley-Woodyear, T.; Wu, Y.; Campbell, C. N.; Heller, A. *J. Am. Chem. Soc.* **1999**, *121*, 10803−10812.
(47) Noy, A.; Vezenov, D. V.; Kayyem, J. F.; Meade, T. J.; Lieber, C. M. *Chem. Biol.* **1997**, *4*, 519−527.
(48) Peterlinz, K. A.; Georgiadis, R. M.; Herne, T. M.; Tarlov, M. J. *J. Am. Chem. Soc.* **1997**, *119*, 3401−3402.
(49) Elghanian, R.; Storhoff, J. L.; Mucic, R. C.; Letsinger, R. L.; Mirkin, C. A. *Science* **1997**, *277*, 1078−1081.
(50) Storhoff, J. J.; Elghanian, R.; Mucic, R. C.; Mirkin, C. A.; Letsinger, R. L. *J. Am. Chem. Soc.* **1998**, *120*, 1959−1964.
(51) Taton, T. A.; Mirkin, C. A.; Letsinger, R. L. *Science* **2000**, *289*, 1757−1760.
(52) Huang, E.; Satiapipat, M.; Han, S.; Zhou, F. *Langmuir* **2001**, *17*, 1215−1224.
(53) Takenaka, S.; Yamashita, K.; Takagi, M.; Uto, Y.; Kondo, H. *Anal. Chem.* **2000**, *72*, 1334−1341.
(54) Hashimoto, K.; Ito, K.; Ishimori, Y. *Anal. Chem.* **1994**, *66*, 3830−3833.
(55) Song, F.; Briseno, A.; Zhou, F. *Langmuir* **2001**, *17*, 4081−4089.

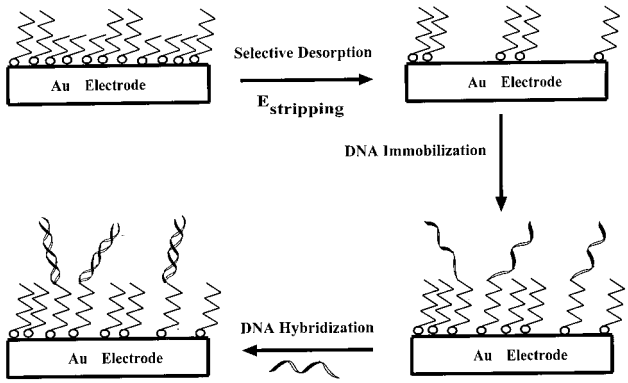

Figure 1. Schematic representation of selective desorption of an alkanethiol in a mixed SAM for subsequent oligonucleotide immobilization and hybridization.

of $\chi_{MPA}/\chi_{MCH} = 1/4$ for the MPA/MCH system were examined. To strip MPA off the substrate, 0.5 M NaOH solution was used as the electrolyte solution. Desorption of MPA was performed with the substrate potential held at −1.0 V for 10 min and monitored simultaneously by AFM. For in-situ monitoring of oligonucleotide immobilization onto the bare gold regions distributed within the HT SAMs, the substrate was rinsed thoroughly with water and mounted onto the AFM liquid cell containing 350 μL of TNE solution. After an AFM image of the MPA-free substrate was collected, 150 μL of a 10 μg/mL probe solution was either carefully pipetted into the cell or injected through a homemade AFM liquid flow cell. The immobilization process was followed continuously for 4 h.

(b) QCM. Mixed MPA/HT or MPA/MCH SAMs on QCM crystals were formed in the same procedure described above. Upon stripping MPA, the crystal containing HT or MCH and freshly exposed gold regions was immersed in 3.21 μg/mL HS-ss-DNA for 4 h. Crystals covered with the newly formed mixed HS-ss-DNA/alkanethiol SAMs were then mounted onto the QCM flow cell for DNA hybridization experiments.

For comparison, hybridization experiments were also performed on mixed HS-ss-DNA/alkanethiol films produced via HS-ss-DNA chemisorption, followed by the competitive alkanethiol replacement procedure. In this procedure, a Au-coated QCM crystal was first soaked in the HS-ss-DNA solution for 4 h, followed by immersion in a given alkanethiol (MCH or HT) solution for 1 h.

3. Results and Discussion

3.1. DNA Immobilization Scheme. Figure 1 shows schematically the steps involved in the selective desorption of an alkanethiol, the attachment of the HS-ss-DNA probe, and the final DNA hybridization experiment. By choosing a stripping potential, $E_{stripping}$, at a value between the reduction potential of the shorter alkanethiol (e.g., MPA) and that of the longer alkanethiol (e.g., HT), the shorter alkanethiol can be stripped, and segregated bare gold regions can be created. Crooks and co-workers have shown that diffusion of the alkanethiol molecules from a densely packed region to a bare Au region created by scanning tunneling microscopic patterning[41] or to an area where fresh Au was exposed by electrocorrosion[42] was slow (e.g., 96 h or longer). Thus the attachment of the HS-ss-DNA probes into the segregated Au regions (which takes only 4 h to densely cover the bare gold regions[22]) will form phase-separated HS-ss-DNA/alkanethiol mixed SAMs. If the bare gold regions have domains that approach the size of the HS-ss-DNA probes, the oligonucleotides would tether onto the surface during the HS-ss-DNA immobilization. It has been noted that the HS-ss-DNA strands can be propped up by the adjacent alkanethiols that are adsorbed after the HS-ss-DNA immobilization, resulting in a HS-ss-DNA surface orientation that is more favorable for the subsequent DNA hybridization.[20−22,43,48] Our approach differs in the order of putting the HS-ss-DNA and the "replacing" alkanethiols onto the surface. In the competitive alkanethiol replacement procedure,[20−22,43,48] the HS-ss-DNA was first attached to the gold surface, followed by soaking the HS-ss-DNA-modified surface in an alkanethiol (e.g., MCH) for a predetermined amount of time (e.g., 1 h). A potential problem is that an extensive soaking of the HS-ss-DNA-covered Au surface in the "replacing" alkanethiol solution (which is necessary for a complete elimination of the nonspecifically adsorbed HS-ss-DNA molecules) can cause indiscriminate substitution of some covalently attached HS-ss-DNA molecules, owing to the stronger affinity of the alkanethiol toward the Au surface. Consequently, the total number of DNA hybridization events per unit area could decrease owing to the partial loss of useful HS-ss-DNA probes. In our methodology, the possible loss of HS-ss-DNA probes is avoided, since the HS-ss-DNA was immobilized in a later step.

Note that in the above scheme, the longer alkanethiol has the same length as the tether group on the oligonucleotide. Matching the lengths of the tether groups has been shown to result in a HS-ss-DNA surface orientation more favorable for the subsequent DNA hybridization.[20−22,47] Recently Demers et al. also showed that extending the tethered DNA probes into the solution with an elongated DNA strand can enhance the DNA hybridization efficiency.[44] In this work, for the purpose of comparing our immobilization scheme to other reports based on alkanethiol-tethered oligonucleotides, we did not investigate the influence of the DNA strand length on the probe surface density and target hybridization efficiency.

The possibility of selectively desorbing an alkanethiol in a binary SAM was first examined using cyclic voltammetry (CV). In the first potential scan (Figure 2a), components of different chain lengths undergo reductive desorption at different potentials (MPA at −0.86 V, MCH at −1.02 V, and HT at −1.13 V). These potentials are essentially identical to the reduction potentials at SAMs of individual alkanethiols. This suggests that there is a high degree of phase separation in the binary SAM.[34,39,56] During the reversal scan of the first cycle, a small amount of desorbed HT or MCH (but not MPA) can be redeposited (Figure 2b). Porter and co-workers have reported similar phenomena in connection with the electrochemical desorption of alkanethiols in alkaline solutions.[37,38,40] Apparently desorption of the more hydrophilic MPA is a faster process. The new reduction peak that appeared at ca. −0.47 V in the second scan is ascribed to the reduction of dissolved oxygen at the freshly exposed Au regions. This peak decreased upon degassing the solution with N_2.

In the mixed SAMs, HT was found to be present at a higher percentage than MPA even if the films were soaked in a $\chi_{MPA}/\chi_{HT} = 1/1$ solution for 12−16 h. This higher percentage of HT is evident in the mass loss shown in Figure 2b. Using the cumulative mass loss estimated from a continuous EQCM monitoring for 15 cycles, the molar ratio between the amount of desorbed MPA and that of desorbed HT was calculated to be around 1/4. This is in line with many other published results,[4,34,37,39,57] which indicated that a longer soaking time favors the adsorption of the longer alkanethiol.

The gold areas freshly exposed can be deduced on the basis of the amount of MPA desorbed and the surface

(56) Nishizawa, M.; Sunagawa, T.; Yoneyama, H. *J. Electroanal. Chem.* **1997**, *436*, 213−218.
(57) Rowe, G. K.; Creager, S. E. *Langmuir* **1994**, *10*, 1186−1192.

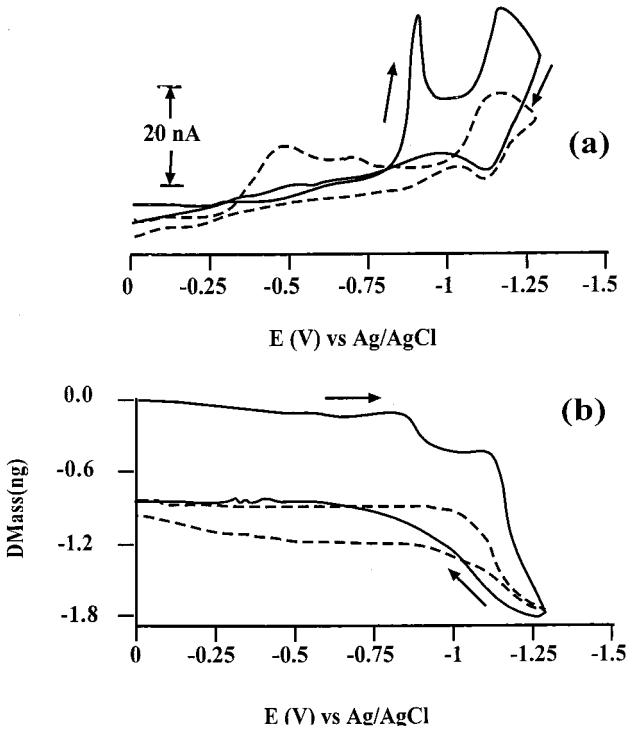

Figure 2. Cyclic voltammograms of a mixed MPA/HT SAM (a) and the frequency changes (b) simultaneously recorded at a Au-coated quartz crystal in a 0.5 M NaOH solution. The first potential cycle is shown as the solid line curve and the second is presented as the dotted line. Arrows indicate the scan directions. The scan rate was 0.05 V/s. The crystal was immersed in a $\chi_{MPA}/\chi_{HT} = 1/1$ solution overnight to form the mixed SAM.

density of a closely packed alkanethiol. Using 7.6×10^{-10} mol/cm^2 expected for the $(\sqrt{3} \times \sqrt{3})R30°$ packing,[58] the gold areas exposed from the three MPA/HT films were calculated to be 0.097 cm^2 ($\chi_{MPA}/\chi_{HT} = 4/1$), 0.079 cm^2 ($\chi_{MPA}/\chi_{HT} = 1/1$), and 0.043 cm^2 ($\chi_{MPA}/\chi_{HT} = 1/4$), which are all smaller than the total area of the substrate (0.259 cm^2).

We performed an electrochemical AFM experiment to monitor the reductive desorption of MPA. Two AFM images of an area that was originally covered with a mixed SAM prepared from a $\chi_{MPA}/\chi_{HT} = 1/4$ solution were shown before (Figure 3a) and after (Figure 3b) the MPA desorption. The difference in the cross-sectional contours between these images shows that reductive desorption of MPA resulted in the disappearance of many small and isolated "islands". The size of these islands, which corresponds to the dimension of the area originally occupied by the MPA molecules, ranges from 12 to 19 nm. The height variation in Figure 3a is about 6−8 Å, whereas that in Figure 3b is about 12−15 Å. These values are in good agreement with the length difference between MPA and HT (4.623 Å if 1.541 Å is used as the C−C bond length[59]) and that between HT and the underlying gold surface (11.06 Å if 1.81 Å is used as the C−S bond length), respectively. The size of the MPA-rich region within a mixed MPA/HT SAM was found to vary with the MPA/HT compositions. These values are comparable to those of the phase-separated 1-hexadecanethiol/MPA[39] and 1-undecanethiol/MPA (10−20 nm) SAMs.[34] On the basis of the consistency between the CV and AFM findings and the agreement of our values with those of other reports, we conclude that phase separation exists in the mixed MPA/HT SAMs at the nanometer scale, and the MPA domains can be altered by varying the soaking solution composition.

3.2. Immobilization of Oligonucleotide Probes onto Gold Regions Dispersed in HT SAMs. We studied the immobilization of HS-ss-DNA onto the freshly exposed gold regions intermixed with HT molecules using FI-QCM. Figure 4 depicts the QCM responses to the immobilization of the HS-ss-DNA probes onto the crystals containing interdispersed gold regions and HT-rich domains. For the 4-min exposure of the Au surface to the injected probe solution, the amount of HS-ss-DNA immobilization increased with the area of gold available. HS-ss-DNA surface densities of 2.64×10^{-12} mol/cm^2 (at films prepared with $\chi_{MPA}/\chi_{HT} = 4/1$), 2.69×10^{-12} mol/cm^2 (at films prepared with $\chi_{MPA}/\chi_{HT} = 1/1$), and 3.56×10^{-12} mol/cm^2 (at films prepared $\chi_{MPA}/\chi_{HT} = 1/4$) were obtained. Exposure of the surface composed of segregated gold and HT regions to the DNA probe solution for 4 h typically increased the amount of HS-ss-DNA immobilized and the surface density by 5−6 times (2.12×10^{-11} mol/cm^2 was observed at a film originally prepared from $\chi_{MPA}/\chi_{HT} = 4/1$). Such a value is in excellent agreement with the surface density of a thiolated 16mer in a mixed SAM containing MCH (about 2.0×10^{-11} mol/cm^2 estimated from Figure 3 in ref 20) and slightly greater than values reported from other QCM measurements (e.g., $\sim 1.5 \times 10^{-11}$ mol/cm^2 in ref 60 and 7.4×10^{-12} mol/cm^2 in ref 14). It is also greater than the value reported by Noy et al. who formed a mixed 16-mercaptohexadecanol/thiolated 14mer using a solution containing both the alkanethiol and the thiolated DNA.[47] Although oligonucleotide surface densities in films created by various immobilization methods cannot be directly compared owing to the differences in the preparative parameters, the types of covalent bonds, and the lengths of oligonucleotides,[20,44,61] the relatively high surface densities suggest that our immobilization scheme is effective. Interestingly, the HS-ss-DNA surface density was the highest when the gold domain was the smallest. This suggests that the steric hindrance caused by the neighboring HT molecules plays an important role in the HS-ss-DNA immobilization. As the gold domains become comparable to the length of the HS-ss-DNA, the nonspecific interactions between the bases on the HS-ss-DNA with the exposed Au regions are most likely minimized. The HS-ss-DNA molecules packed in such a spatially congested area should adopt an orientation in which the DNA strands extend into the solution. This configuration is essentially the same as that in the mixed HS-ss-DNA/MCH SAMs fabricated by the competitive alkanethiol replacement procedure.[20−22,43,48]

To understand the surface orientation of HS-ss-DNA distributed within the HT matrix, we used AFM to monitor the probe immobilization process. Figure 5a depicts an AFM image of a surface covered by a mixed HS-ss-DNA/HT SAM. This surface was produced by exposing a substrate with segregated Au regions distributed in a HT medium in a HS-ss-DNA solution for 4 h. The average HS-ss-DNA surface density, deduced by counting the molecules across a unit area from three different measurements, was 1.22×10^{-14} mol/cm^2.

While it is conceivable that the distribution of the segregated gold regions governs the uniformity of the probe immobilization, the influence of the domain size of the gold region on the probe orientation is not obvious.

(58) Wildrig, C. A.; Alves, C. A.; Porter, M. D. *J. Am. Chem. Soc.* **1991**, *113*, 2805−2810.
(59) Leung, T. Y. B.; Gerstenberg, M. C.; Lavrich, D. J.; Scoles, G. *Langmuir* **2000**, *16*, 549−561.
(60) Okahata, Y.; Kawase, M.; Niikura, K.; Ohtake, F.; Furusawa, H.; Ebara, Y. *Anal. Chem.* **1998**, *70*, 1288−1296.
(61) Huang, E.; Zhou, F.; Deng, L. *Langmuir* **2000**, *16*, 3272−3280.

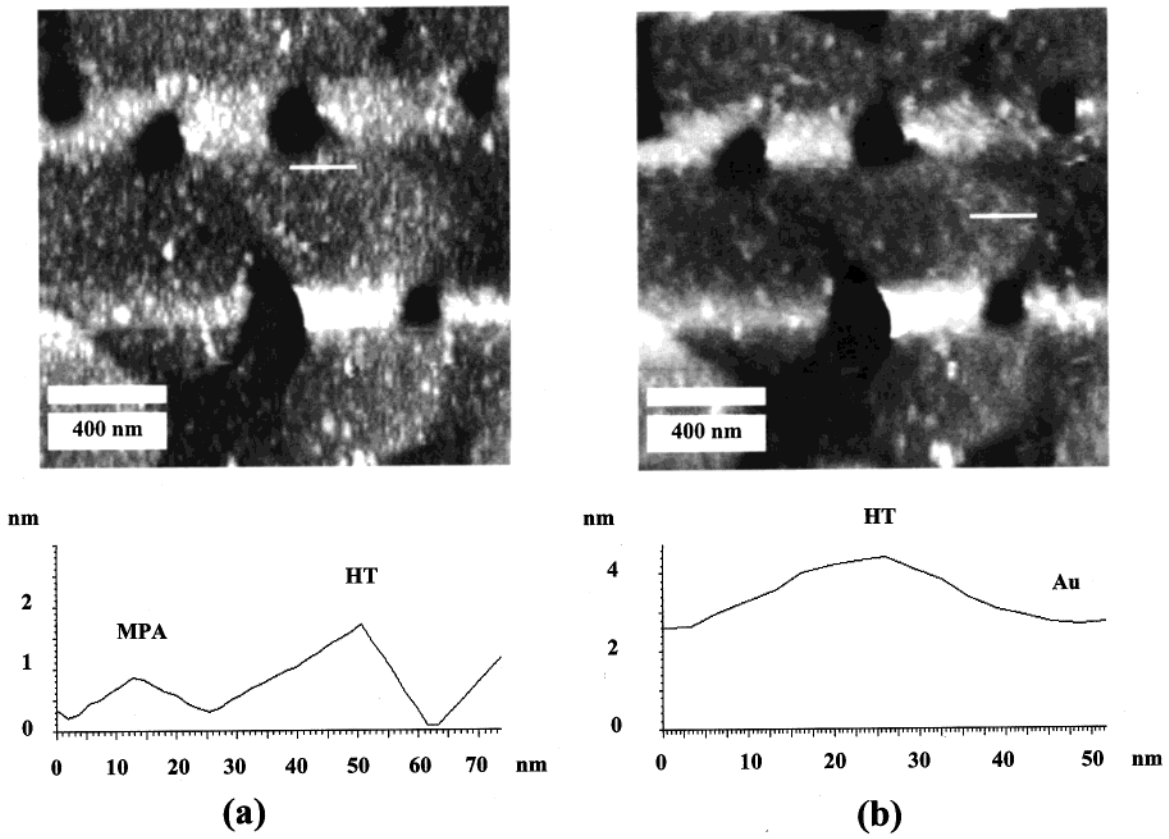

Figure 3. Topographical AFM images of a mixed MPA/HT SAM formed from a $\chi_{MPA}/\chi_{HT} = 4/1$ solution (a) and the same area after the MPA had been desorbed at −1.0 V for 10 min in a 0.5 M NaOH solution (b).

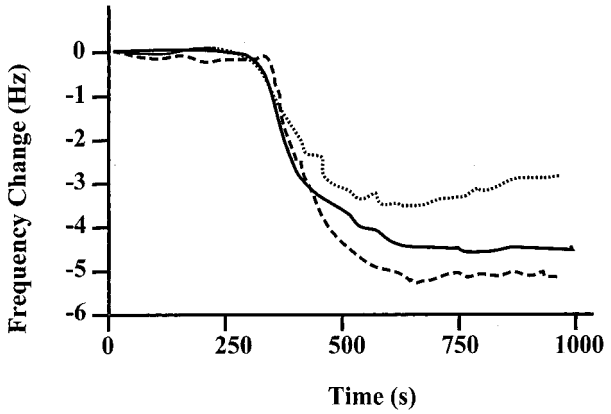

Figure 4. QCM responses to the injections of 100 μL of TE solutions containing 3.21 μg/mL HS-ss-DNA into a flow cell housing Au-coated crystals covered with different amounts of HT prepared from solutions of $\chi_{MPA}/\chi_{HT} = 4/1$ (dashed line curve), $\chi_{MPA}/\chi_{HT} = 1/1$ (solid line curve), and $\chi_{MPA}/\chi_{HT} = 1/4$ (dotted line curve).

Fortunately, this issue can also be addressed conveniently by AFM. Table 1 summarized the HS-ss-DNA surface densities and the diameters and heights of the surface-confined HS-ss-DNA molecules in different types of HS-ss-DNA SAMs or mixed SAMs. We should note that the discrepancy in the values deduced from the AFM and QCM measurements has been attributed to the difference in the gold grain sizes between the AFM substrate and the QCM crystal.[52] Other researchers have also observed that a surface containing smaller Au grains facilitates the adsorption of a larger number of alkanethiol molecules.[62] Shown in Figure 5b is an AFM image of the probes distributed within a SAM of a higher HT surface coverage (using a $\chi_{MPA}/\chi_{HT} = 1/4$ solution). While Figure 5a and b shows uniform probe distributions, the average height difference between the HS-ss-DNA probes and the underlying HT molecules in Figure 5b (3.5−5.5 nm) is much greater than that in Figure 5a (1.7−2.5 nm). The 17mer, if completely extended, should have a length of 5.78 nm.[63] Therefore, it is clear from Table 1 that the oligonucleotide probes are extended to a greater extent in a more sterically restricted area. The HS-ss-DNA surface density in a HS-ss-DNA/MCH mixed SAM fabricated using our method ($(2.0 \pm 0.3) \times 10^{-14}$ mol/cm^2, image not shown) is comparable to that in the HS-ss-DNA/MCH SAM, but the average height is less (~4 nm). This is not surprising considering that other studies have demonstrated that OH-terminated SAMs are more defective and less well-ordered than the CH_3-terminated SAMs.[64] In other words, the more densely packed HT molecules would prop up the HS-ss-DNA molecules more significantly.

We should note that, while the MAC-AFM mode is very gentle for imaging biological molecules, some compression of these surface-confined oligonucleotide molecules might have occurred. Thus the actual heights might be higher than those listed in Table 1. Moreover, the molecules in the more loosely packed domains, which experience a smaller steric hindrance than those in the more densely packed areas, could be more compressed by the AFM tip. Nevertheless, this effect is probably not large enough to account for the obvious height difference shown in Table 1.

(62) Thomas, R. C.; Yang, H. C.; DiRubio, C. R.; Ricco, A. J.; Crooks, R. M. *Langmuir* **1996**, *12*, 2239−2246.

(63) Lehninger, A. L.; Nelson, D. L.; Cox, M. M. *Principles of Biochemistry*; Worth Publishers: New York, 1993.

(64) Chidsey, C. E. D.; Loiacono, D. N. *Langmuir* **1990**, *6*, 682−691.

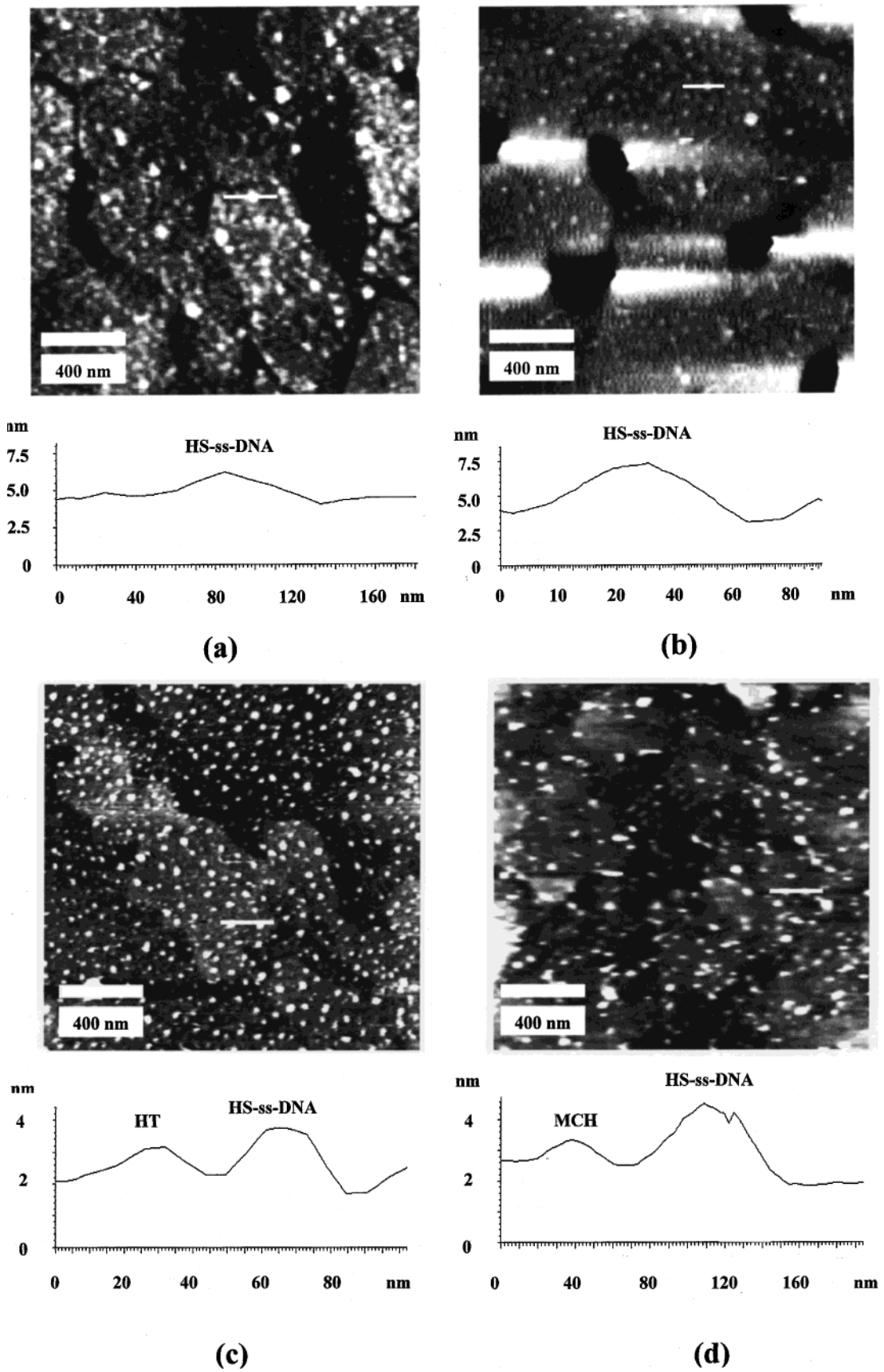

Figure 5. Topographical AFM images showing the immobilization of HS-ss-DNA probes at surfaces with different HT coverages. Image a was collected 4 h after a surface containing freshly exposed Au regions segregated in a HT SAM (from a solution of $\chi_{MPA}/\chi_{HT} = 1/1$) had been exposed to a HS-ss-DNA solution. Image b shows a mixed HS-ss-DNA/HT SAM prepared similarly to image a, except that a $\chi_{MPA}/\chi_{HT} = 1/4$ solution was used. Images c and d are the mixed HS-ss-DNA/HT and HS-ss-DNA/MCH SAMs prepared by immersion of the Au substrates for 4 h in a HS-ss-DNA solution, followed by 1 h of soaking in 1 mM of the respective alkanethiol solutions.

Table 1. Averaged Surface Density, Diameters, and Heights of HS-ss-DNA in Different SAMs Measured by AFM[a]

	SAMs					
parameters	HS-ss-DNA	HS-ss-DNA/MCH	HS-ss-DNA/HT	HS-ss-DNA/HT χ_{HT}/χ_{MP}[c] = 4/1	HS-ss-DNA/HT χ_{HT}/χ_{MPA} = 1/1	HS-ss-DNA/HT χ_{HT}/χ_{MPA} = 1/4
density ($\times 10^{-15}$ mol/cm^2)	18.3 ± 5.0	5.5 ± 0.1	14.0 ± 4.0	19.0 ± 9.0	8.2 ± 0.4	6.2 ± 0.4
height (nm)[b]	1.8 ± 0.5	2.2 ± 0.4	2.1 ± 0.2	4.5 ± 1.0	2.1 ± 0.4	1.8 ± 0.4
diameter (nm)	19−42	28−39	15−33	12−28	17−34	23−42

[a] Average of three measurements. [b] Weighted average of different heights. [c] Solution composition for the mixed SAM formation.

We contrasted the probe coverage and orientation in Figure 5b to that immobilized via simple chemisorption. Previously, we have estimated a thiolated 17mer surface coverage to be 1.83×10^{-14} mol/cm^2 with a large size variation[52] (19−42 nm in Table 1). Based on the model proposed by Tarlov and co-workers, while some of the probes are tethered, many others will lean toward the substrate.[20−22,43,48] This is in sharp contrast to the narrow range in Figure 5b (12−28 nm). The steric congestion in a highly localized area thus reduces the variation of the cross sections of the DNA strands.

Finally, we compared the surface coverage and orientation of the HS-ss-DNA molecules in the mixed SAMs prepared using our method to that fabricated by the competitive alkanethiol replacement procedure. Figure 5c is an image of a HS-ss-DNA/HT SAM, and Figure 5d shows a HS-ss-DNA/MCH SAM. The HS-ss-DNA surface density estimated from Figure 5c (1.40×10^{-14} mol/cm^2) and that deduced from Figure 5d (5.5×10^{-15} mol/cm^2) are both smaller than the value in Figure 5b (1.90×10^{-14} mol/cm^2) and that associated with the 17mer SAM (1.83×10^{-14} mol/cm^2),[52] suggesting that a large number of HS-ss-DNA molecules have been substituted by the "replacing" alkanethiol in the solution. This observation is in line with the QCM results described in the following section.

3.3. DNA Target Hybridization with HS-ss-DNA Probes in Various Mixed SAMs. To demonstrate that the mixed HS-ss-DNA/alkanethiol SAMs prepared by our method are useful for DNA hybridization, we carried out several DNA hybridization assays. The resolution of our AFM tips is not high enough to resolve ds-DNA from ss-DNA. Therefore, we relied on FI-QCM, since it can gauge the hybridization process across the entire sensing surface. It is known that QCM is not very sensitive for the detection of oligonucleotide hybridization without signal amplification, when the number of probes at the surface is limited and the target in the solution is of a low concentration.[28,65] As shown below, the mixed HS-ss-DNA/alkanethiol SAMs with a denser surface coverage and a more favorable probe orientation help enhance the QCM detection of DNA hybridization.

Figure 6 shows a series of QCM frequency decreases (mass increases) to target hybridization at crystals covered with different types of mixed HS-ss-DNA/alkanethiol SAMs. Curve a, acquired at a binary HS-ss-DNA/HT SAM prepared with our method, yielded the highest frequency decrease (17 Hz). This is in contrast with the response in curve c obtained at a mixed HS-ss-DNA/HT SAM produced by the competitive alkanethiol replacement procedure (ca. 7 Hz). Similarly, the frequency decrease at the mixed HS-ss-DNA/MCH SAM prepared with the present method (9.6 Hz in curve b) was also found to be greater than that at its counterpart fabricated by the competitive alkanethiol replacement procedure (about 3 Hz in curve d). Clearly, all the frequency decreases in curves a−d were greater than that recorded at the SAM of only HS-ss-DNA (1.8 Hz in curve e), suggesting that our method and the competitive alkanethiol replacement procedure both produce surfaces with more HS-ss-DNA probes adopting the orientation favorable for hybridization. Considering that the DNA surface densities at films for curves a and c are similar (see the AFM results presented in section 3.2), the greater QCM frequency decrease at the HS-ss-DNA/HT SAM (curve a) must result from the more favorable HS-ss-DNA surface orientation.

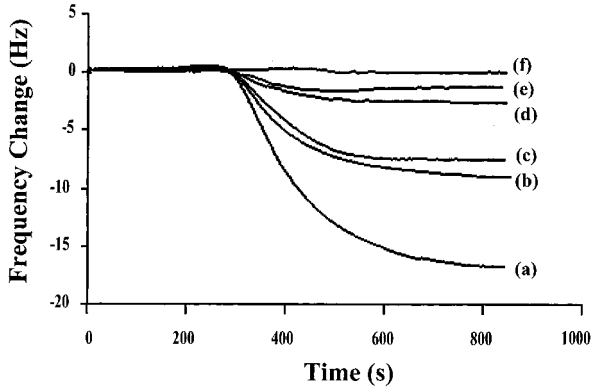

Figure 6. QCM responses to the injections of 100 μL of a 3.35 μg/mL target solution at various HS-ss-DNA SAMs or HS-ss-DNA/alkanethiol mixed SAMs: (a) a HS-ss-DNA/HT SAM prepared with the present method (the original soaking solution had a composition of $\chi_{MPA}/\chi_{HT} = 1/4$), (b) a mixed HS-ss-DNA/MCH prepared as in (a) except that MCH, instead of HT, was used, (c) a mixed HS-ss-DNA/HT produced by the competitive alkanethiol replacement procedure, (d) a mixed HS-ss-DNA/MCH, also formed by the competitive alkanethiol replacement procedure, (e) a Au surface covered with only the HS-ss-DNA probes, and (f) a mixed SAM-containing HT and a thiolated 15mer whose sequence mismatches the target sequence, formed using the present method.

The QCM signal enhancements at the mixed HS-ss-DNA/HT SAMs prepared using solution compositions of $\chi_{MPA}/\chi_{HT} = 1/1$ and $\chi_{MPA}/\chi_{HT} = 4/1$, on the other hand, are not significant. The average frequency changes at mixed HS-ss-DNA/HT SAMs from $\chi_{MPA}/\chi_{HT} = 1/1$ and from $\chi_{MPA}/\chi_{HT} = 4/1$ were about 3.3 and 2.4 Hz, respectively.

To verify the absence of nonspecific adsorption of DNA targets at the various surfaces, we performed a control experiment, and the result is shown as curve f in Figure 6. The introduction of the target into the cell housing the crystal covered with a mixed SAM of HT and a non-complementary HS-ss-DNA did not produce any discernible frequency change, suggesting that nonspecific DNA adsorption did not take place at the binary HS-ss-DNA/HT SAMs.

The hybridization efficiencies at some of these films can be estimated. The immobilization of the 17mer HS-ss-DNA onto a Au surface typically yielded a frequency decrease of about 12.5 Hz (2.5 pmol).[52] To verify whether all of the useful probes on the entire sensing surface had been fully hybridized with the target, we carried out another injection after acquiring curve e in Figure 6 and

(65) Han, S.; Lin, J.; Satjapipat, M.; Baca, A. J.; Zhou, F. *Chem. Commun.* **2001**, 609−610.

observed a frequency decrease of ca. 0.5 Hz (data not shown). The third injection did not yield any signal above the baseline. The cumulative target hybridized was then calculated to be 0.49 pmol. Thus the overall hybridization efficiency should be (0.49 pmol/2.5 pmol) × 100% = 19.6%. Since AFM revealed that about 17% of the probes were tethered in the HS-ss-DNA SAM (heights greater than 2 nm), it appears that only these probes had been utilized during the DNA hybridization. The hybridization efficiency at the mixed HS-ss-DNA/HT SAM prepared with our method, on the other hand, is much higher. As mentioned above, the 4-h exposure of the segregated gold regions to a HS-ss-DNA solution resulted in an averaged frequency change of about 20.8 Hz (4.25 pmol). As for the target hybridization, the cumulative frequency decrease and the total hybridized target from three consecutive injections were 19.1 Hz or 4.06 pmol, respectively (averaged from three measurements). Therefore, the overall hybridization efficiency at the mixed HS-ss-DNA/HT SAMs prepared with our method is (4.06 pmol/4.25 pmol) × 100% = 95.5%. A high overall hybridization efficiency (∼80%), which is consistent with that reported by Tarlov and co-workers,[20−22,43] was also observed for the HS-ss-DNA/MCH binary SAM system.

The hybridization efficiencies associated with curves c and d, on the other hand, are difficult to estimate because QCM only measures a net mass change at the surface. The attachment of HT or MCH increases the mass change while the loss of the replaced HS-ss-DNA reduces the mass at the crystal surface. Therefore, the actual amount of HS-ss-DNA present at the surface cannot be measured. Unfortunately, the surface densities of HS-ss-DNA/HT or HS-ss-DNA/MCH deduced from the AFM experiments are not applicable because of the aforementioned morphological difference between the AFM gold substrate and the gold film on the QCM crystal.[52] The validity of the Sauerbrey equation for the quantitative interpretation of the QCM results might also be an issue.[66−68] Although the tethered HS-ss-DNA molecules are short and do not extend beyond the surface acoustic wave launched at the crystal surface (typically a few micrometers[68]), they cannot be simply regarded as rigidly bound molecules. Furthermore, DNA molecules are highly solvated.[63] Therefore, the viscoelastic effects cannot be completely ignored, making the results calculated by the Sauerbrey equation semiquantitative at best. Nevertheless, QCM is a technique complementary to AFM for the purpose of studying probe immobilization and target hybridization, since it can provide a descriptive and semiquantitative interpretation about the extents of the probe immobilization and the DNA hybridization across the entire sensing surface.

4. Conclusion

A method for immobilizing HS-ss-DNA probes with a high surface density and a surface orientation optimal for DNA hybridization has been developed. Gold regions freshly exposed by selective desorption of a shorter alkanethiol in a mixed SAM can be used as sites for attaching HS-ss-DNA. CV and AFM indicate that the gold regions are segregated from the remaining alkanethiol molecules of a longer chain length (e.g., hexanethiol, HT). The sizes of these sites can be varied by altering the solution composition initially used to form the mixed SAMs. The surface density of HS-ss-DNA begins to increase when the domains of the segregated gold regions become comparable to the size of the HS-ss-DNA. This increase in surface density (a decrease in the number of nonspecifically adsorbed HS-ss-DNA and an increase in the total amount of tethered HS-ss-DNA) is ascribed to the surface reorientation of the HS-ss-DNA probes. The tethered HS-ss-DNA molecules are known to be more favorable for DNA hybridization. The surface density of HS-ss-DNA in the mixed HS-ss-DNA/alkanethiol SAMs prepared via the sequential adsorptions of HS-ss-DNA and a "replacing" alkanethiol, on the other hand, is several times smaller. Our immobilization method avoids the indiscriminate replacement of the DNA probes by the "replacing" alkanethiol, an aspect inherent in the competitive alkanethiol replacement procedure, and makes the FI-QCM detection of the oligonucleotide target more sensitive. The QCM signal intensity was amplified by almost 1 order of magnitude when compared to that at SAMs containing only the HS-ss-DNA probes and by 2−3 times when compared to that at mixed SAMs formed with the competitive alkanethiol replacement procedure. The overall hybridization efficiency was estimated to increase from 19.6% at the HS-ss-DNA SAMs to 95.5% at the mixed HS-ss-DNA/HT SAMs prepared with our method.

Acknowledgment. Support for this work by the NIH-SCORE subproject (GM08101), the donors of the Petroleum Research Fund administered by the American Chemical Society, the NSF-CRUI project (DBI-9978806), and the NSF-CEA-CREST program is gratefully acknowledged.

LA010989I

(66) Thompson, M.; Stone, D. C. *Surface-Launched Acoustic Wave Sensors*; John Wiley & Sons: New York, 1990.

(67) Dunham, G.; Benson, N. H.; Danuta, P.; Janata, J. *Anal. Chem.* **1995**, *57*, 267−272.

(68) Fawcett, N. C.; Craven, R. D.; Zhang, P.; Evans, J. A. *Anal. Chem.* **1998**, *70*, 2876−2880.